NASA TECHNICAL MEMORANDUM

NASA TM X-1067

NASA TM X-1067

EFFEC[redacted]
ON S[redacted]
VELO[redacted]
BLUN[redacted]

by Ern[redacted]

Langle[redacted]
Langle[redacted]

NATIONAL A[redacted]

[redacted]

NASA TM X-1067

DECLASSIFIED.
AUTHORITY. US 663
DROBKA TO LEBOW MEMO DATED.
JAN.10, 1966

EFFECTS OF CORNER RADIUS ON STAGNATION-POINT VELOCITY GRADIENTS ON BLUNT AXISYMMETRIC BODIES

By Ernest V. Zoby and Edward M. Sullivan

Langley Research Center
Langley Station, Hampton, Va.

Declassified by authority of NASA
Classification Change Notices No. 50
Dated 2/16/66

C65-2713

[redacted]

[redacted]

NATIONAL AERONAUTICS AND SPACE ADMINISTRATION

[redacted]

[redacted]

EFFECTS OF CORNER RADIUS ON STAGNATION-POINT VELOCITY GRADIENTS ON BLUNT AXISYMMETRIC BODIES*

By Ernest V. Zoby and Edward M. Sullivan
Langley Research Center

SUMMARY

27043

Results of an analytical study initiated to determine the effects of corner radius on stagnation-point velocity gradients on blunt bodies at a 0° angle of attack are presented. The blunt bodies investigated included a range of ratios of body radius to nose radius r_B/r_N from 0 (flat-faced cylinder) to 1.0 (hemisphere) and ratios of corner radius to body radius from 0 (sharp corner) to 0.3.

The velocity gradients on the blunt bodies were calculated from published experimental pressure distributions with the aid of the thermodynamic properties of equilibrium air and isentropic flow relationships.

For a r_B/r_N ratio less than 0.5, increasing the corner radius increases the velocity gradient and thus increases the stagnation-point heating rate. These effects become more pronounced with increasing nose radius. For a r_B/r_N ratio greater than 0.5, the corner radius has a negligible effect on the velocity gradient for the range of corner-radius ratios investigated.

Conf

INTRODUCTION

Author 1

One of the problems encountered in the application of stagnation-point heat-transfer theories (e.g., refs. 1 and 2) is the calculation of the stagnation-point velocity gradient $(dU/dS)_s$. For the particular case of a hemispherical nose, Fay and Riddell (ref. 1) and others show that $(dU/dS)_s$ can be evaluated from Newtonian flow. Boison and Curtiss (ref. 3) have experimentally determined $(dU/dS)_s$ for a family of sharp-cornered blunt axisymmetric noses on cylinders.

Some theoretical work showing the relationship between $(dU/dS)_s$ on a blunt body with sharp corners and $(dU/dS)_s$ on a hemisphere has been published.

*Title, Unclassified.

[redacted]

(See ref. 4.) This work is based on the proportionality between the stagnation-point heating rate and the square root of the stagnation-point velocity gradient, where $(dU/dS)_s$ is determined from the pressure distribution over the body. In reference 4, the pressure distribution was assumed to be a function only of geometry for $M \gtrsim 2.0$. Recent experimental pressure data obtained in the Langley Unitary Plan wind tunnel indicate that the pressure distribution is invariant for $M \gtrsim 3.5$. Experimental evidence can be found for $M > 6.0$ in reference 5 and for Mach numbers from 3.0 to 24.4 over a Reynolds number range of 0.052×10^6 to 4.22×10^6 in reference 6.

The present report presents the results of an analytical investigation of the effects of corner radius on the stagnation-point velocity gradient. The results are presented as plots of $\sqrt{\frac{(dU/dS)_{s,BB}}{(dU/dS)_{s,Hemi}}}$ for the range of blunt bodies between a flat face $\left(\frac{r_B}{r_N} = 0\right)$ and a hemisphere $\left(\frac{r_B}{r_N} = 1.0\right)$. Stoney initiated this procedure in reference 4. Corner radii up to 0.3 of the body radii have been included. Also, as in reference 3, the correlation between the velocity gradient and the effective radius $\left(r_{eff}\right)$ has been established and the parameter r_B/r_{eff} has been incorporated in the presentation of the results.

SYMBOLS

a	speed of sound, ft/sec
g,f	functional relationships (eqs. (1) and (2))
h	heat-transfer coefficient, Btu/ft^2-sec-$^\circ$R
M	Mach number
p	pressure, lbf/ft^2
$\dot{q}$	heat-transfer rate, Btu/ft^2-sec
r_B	body radius (fig. 1), ft
r_C	corner radius (fig. 1), ft
r_{eff}	"effective" radius (eqs. (4) and (5)), ft
r_N	nose radius (fig. 1), ft
S	distance from stagnation point along surface, ft

[redacted]

T	temperature, $^{\circ}R$
U	velocity, ft/sec
dU/dS	velocity gradient, sec^{-1}
γ_{eff}	real-gas isentropic exponent $\left(a^2 \frac{\rho_s}{p_s}\right)$
ρ	density, slugs/ft^3

Subscripts:

2	condition behind normal shock
∞	free stream
e	edge of boundary layer
s	stagnation point
t	total conditions
a,b	different body sizes
BB	blunt body
Hemi	hemisphere of radius r_B
exp	experimental

ANALYSIS

The velocity gradient is a function of all the flow parameters which influence the local velocity in the stagnation region, including dissociation and ionization. However, if equilibrium air properties and isentropic flow are assumed, the velocity gradient is a function of flight conditions and the pressure gradient and can be written as

$$\left(\frac{dU}{dS}\right)_s = g\left(p_{t,2}, T_{t,2}, \frac{dp}{dS}\right) \tag{1}$$

Also, since the flow in the stagnation region of a blunt body will be the same as the flow in the stagnation region of a hemisphere at the same flight conditions, except for pressure distribution effects, it follows that

$$\frac{(dU/dS)_{s,BB}}{(dU/dS)_{s,Hemi}} = f\left[\frac{(dp/dS)_{s,BB}}{(dp/dS)_{s,Hemi}}\right] \tag{2}$$

The application of the assumption that the pressure distribution is a function of geometry (i.e., the pressure distribution is fixed on the body) for $M \gtrsim 3.5$ can be used to establish that $(dp/dS)_{s,BB}$ and $(dp/dS)_{s,Hemi}$ are both constant. Hence, the functional relationship (f of eq. (2)) must also be constant for all flight conditions where $M \gtrsim 3.5$.

Thus, if the pressure distribution on a body is known for flight conditions where $M \gtrsim 3.5$, and if the functional relationship g is known, the stagnation-point velocity gradient can be found (eq. (1)). Further, the results of the analysis can be presented in a readily usable form as a ratio of the calculated blunt-body velocity gradient to the velocity gradient on a hemisphere for which the velocity-gradient calculations are well established.

Boison and Curtiss (ref. 3) have shown that for blunt bodies of the type being considered herein, the velocity gradient in the stagnation region is constant, as though it were the velocity gradient on a hemisphere; that is, the stagnation-region pressure distribution on a blunt body is the same as that found on a hemisphere of some "effective" radius. The "effective" radius is the equivalent hemispherical radius which will produce the same velocity gradient as that computed for the blunt body. Then, since for a hemisphere,

$$\left(\frac{dU}{dS}\right)_{s,Hemi} \approx \frac{1}{r_B}\sqrt{\frac{2p_s}{\rho_s}} \quad \text{(Newtonian flow)} \tag{3}$$

it follows that

$$\left(\frac{dU}{dS}\right)_{s,BB} \approx \frac{1}{r_{eff}}\sqrt{\frac{2p_s}{\rho_s}} \tag{4}$$

and

$$\frac{r_B}{r_{eff}} = \frac{(dU/dS)_{s,BB}}{(dU/dS)_{s,Hemi}} \tag{5}$$

METHOD

The analysis indicates that if the pressure distribution on a body is known, the velocity gradient can be established by evaluation of the functional relationship in equation (2). However, the functional relationship cannot be evaluated directly; therefore the following method was used to calculate the velocity gradients for the purposes of this report.

First, a study of available data was made to obtain experimentally determined pressure distributions over bodies of the type being considered. For a specific body, the pressure data at the highest Mach number were used. The data selected were found in references 3, 5, and 7 to 12.

The pressure distribution for each of the bodies selected, including the hemisphere, was reduced to the form $p_e/p_{t,2}$ as a function of S/r_B. Then a set of flight conditions, U_∞ and ρ_∞, were arbitrarily selected and the flow conditions $\left(p_{t,2}, \rho_{t,2}\right)$ behind the normal portion of the bow shock were determined from the tables in references 13 and 14. These tables are based on air in chemical equilibrium. The velocity was calculated for several points around the body by using the known pressure distribution, the isentropic flow relations, the adiabatic energy equations, and the value of γ_{eff} determined from reference 15 for the stagnation-point conditions. Ratios of these velocities to the free-stream velocity were made, and these ratios were plotted as a function of S/r_B. Figure 2 presents some typical velocity distributions in the stagnation region of some of the blunt bodies at an arbitrarily chosen free-stream velocity of 23 800 ft/sec and an altitude of 138 000 ft. For all cases computed, the ratio of U_e/U_∞ was a linear function of S/r_B in the stagnation region, and the slope of the line (the desired velocity gradient) was graphically determined. The ratio

$$\left[\frac{d\left(U_e/U_\infty\right)}{d\left(S/r_B\right)}\right]_{BB}\Bigg/\left[\frac{d\left(U_e/U_\infty\right)}{d\left(S/r_B\right)}\right]_{Hemi} \tag{6}$$

was then evaluated. Several calculations were then made for some of the bodies at different flight conditions, and as the analysis had predicted, the ratio of expression (6) was constant for each body if the pressure distribution was assumed to be invariant. Thus, an effective radius could be found since this ratio is equivalent to r_B/r_{eff}. Finally, since the free-stream velocity and the body radius will cancel in the numerator and denominator of expression (6), the ratio can be rewritten as

$$\frac{\left(dU_e/dS\right)_{BB}}{\left(dU_e/dS\right)_{Hemi}}$$

RESULTS

The results of this investigation are presented in figures 3 and 4. Faired curves of $(dU/dS)_s$ are presented as a function of the blunt-body parameters r_B/r_N and r_C/r_B for a 0° angle of attack. $\left(\text{By definition } \frac{r_B}{r_N} = 0\right.$ is a flat-faced cylinder, $\frac{r_B}{r_N} = 1.0$ is a hemisphere, and $\frac{r_C}{r_B} = 0$ is a sharp $\left.\text{corner.}\right)$

For heat-transfer calculations the important parameter is $(dU/dS)_s^{1/2}$. Thus figure 3 shows

$$\left[\frac{(dU/dS)_{s,BB}}{(dU/dS)_{s,Hemi}}\right]^{1/2}$$

which for a given set of flight conditions is equal to the ratio $\left(\dot{q}_{BB}/\dot{q}_{Hemi}\right)_s$. Figure 3 shows that for $\frac{r_B}{r_N} \gtrapprox 0.5$, there are no significant effects due to the corner radius over the range of r_C/r_B under consideration, and for $\frac{r_B}{r_N} \lessapprox 0.5$, the effects of corner radius increase as r_B/r_N approaches 0. At $\frac{r_B}{r_N} = 0$, the value of the ordinate increases by approximately 11 percent as the corner-radius ratio increases from 0 to 0.3. It should be noted that the results of the present work for the sharp-cornered bodies $\frac{r_C}{r_B} = 0$ when put in heat-transfer ratio form are in excellent agreement with results of reference 4. Since the amount of pressure data for $M_\infty \gtrapprox 3.5$ available for these blunt bodies was limited, the data for $\frac{r_B}{r_N} = 0$ and $\frac{r_C}{r_B} = 0.333$ at $M_\infty = 2.2$ were included in this paper. For a sharp-cornered body at this low Mach number, the use of this pressure distribution might be questioned. However, this body had a fairly large corner-radius ratio and thus the pressure distribution was assumed to be invariant for $M_\infty < 3.5$.

The results shown in figure 3 have been compared with experimental results from references 16 and 17 for flat-faced bodies with varying corner-radius ratios. The experimental heating rates are approximately 2 percent greater than those in figure 3.

The results of figure 3 are replotted in figure 4 in terms of $\frac{(dU/dS)_{s,BB}}{(dU/dS)_{s,Hemi}}$ and r_B/r_{eff} which have been shown to be equivalent in the analysis section. Since the ordinate is the square of the ordinate in figure 3, the effect of the corner radius is to increase the velocity-gradient ratio by approximately 22 percent at $\frac{r_B}{r_N} = 0$.

APPLICATION OF RESULTS

Use of Velocity-Gradient Curves

The results given in figures 3 and 4 are directly applicable provided the velocity gradient on the hemisphere is known. As previously shown this velocity gradient can be evaluated from equation (3), where p_s and ρ_s must be evaluated from the flow conditions behind the normal part of the bow shock wave. Figure 5, based on the WADC 1959 model atmosphere (ref. 18), has been prepared to facilitate the velocity-gradient calculations. From this figure $\left[\frac{\Delta\left(\frac{U}{U_\infty}\right)}{\Delta\left(\frac{S}{r_B}\right)}\right]_s$ can be determined for a given free-stream velocity and altitude. Then since the free-stream velocity and the body radius are known,

$$\left(\frac{\Delta U}{\Delta S}\right)_{s,Hemi} = \left(\frac{dU}{dS}\right)_{s,Hemi}$$

can be found.

Stagnation-Point Heating

If the stagnation-point heating rate $\dot{q}_s$ is known (see, for example, ref. 2) on a hemisphere of any size at a desired velocity and altitude, the results of figure 2 can be used to evaluate the heating on a blunt body at the same velocity and altitude. The known $\dot{q}_{s,b}$ is simply converted to the $\dot{q}_{s,a}$ on a hemisphere of the desired body radius by the relationship $\frac{\dot{q}_{s,a}}{\dot{q}_{s,b}} = \sqrt{\frac{r_{B_b}}{r_{B_a}}}$ since the $\dot{q}_s$ on a hemisphere is inversely proportional to $\sqrt{r_B}$. Then, from figure 3 the desired $\left(\frac{\dot{q}_{BB}}{\dot{q}_{Hemi}}\right)_s$ can be found and the resultant $\dot{q}_{s,BB}$ can be calculated.

The Effective Radius

The stagnation-point heating-rate theories of Detra, Kemp, and Riddell (ref. 19) and Kemp and Riddell (ref. 20) can be used to obtain values of the stagnation-point heating rates on a hemispherical nose $\left(r_N = r_B\right)$. However, these theories are not directly applicable if r_N does not equal r_B. If the "effective" radius r_{eff} is used as the radius of the hemispherical nose, these theories can be used to calculate the stagnation-point heating rate on a blunt body.

The "effective" radius should also be very useful when an attempt is made to compare experimental and theoretical stagnation-point heat transfer on a blunt body. For example, in figure 9(a) of reference 5, a comparison is made between the measured stagnation-point heat-transfer coefficient on a blunt body and the calculated theoretical heat-transfer coefficient on a hemisphere. The authors show that $\frac{h_{s,exp}}{h_{s,Hemi}}$ is 1.22 where $h_{s,Hemi}$ was based on the nose radius of the blunt body and not on the body radius, as the notation of the present report would indicate. If they had instead chosen to represent their results as $\frac{h_{s,exp}}{h_{s,BB}}$ by using the effective radius of the blunt body, the ratio would have been 1.0.

CONCLUDING REMARKS

Results of an analytical study initiated to determine the effects of corner radius on blunt-body stagnation-point velocity gradients are presented. The velocity gradients were calculated from published experimental pressure distributions with the aid of the thermodynamic properties of equilibrium air and isentropic flow relationships.

Ratios of corner radius to body radius r_C/r_B from 0 to 0.3 were investigated. For this range and for a given ratio of body radius to nose radius r_B/r_N less than 0.5, increasing the corner radius increases the velocity gradient and hence increases the stagnation-point heating rate. These effects become more pronounced with increasing nose radius. For a r_B/r_N ratio greater than 0.5, the corner radius has a negligible effect on the velocity gradient.

Langley Research Center,
National Aeronautics and Space Administration,
Langley Station, Hampton, Va., November 16, 1964.

REFERENCES

1. Fay, J. A.; and Riddell, F. R.: Theory of Stagnation Point Heat Transfer in Dissociated Air. J. Aeron. Sci., vol. 25, no. 2, Feb. 1958, pp. 73-85, 121.

2. Cohen, Nathaniel B.: Boundary-Layer Similar Solutions and Correlation Equations for Laminar Heat-Transfer Distribution in Equilibrium Air at Velocities up to 41,100 Feet Per Second. NASA TR R-118, 1961.

3. Boison, J. C.; and Curtiss, H. A.: Preliminary Results of Spherical-Segment Blunt Body Pressure Surveys in the 20 Inch Supersonic Wind Tunnel at JPL. RAD Tech. Memo 2-TM-57-77 (Aerod. Sec. Memo No. 152), AVCO Res. and Advanced Dev. Div., Oct. 9, 1957.

4. Stoney, William E., Jr.: Aerodynamic Heating of Blunt Nose Shapes at Mach Numbers up to 14. NACA RM L58E05a, 1958.

5. Holloway, Paul F.; and Dunavant, James C.: Heat-Transfer and Pressure Distributions at Mach Numbers of 6.0 and 9.6 Over Two Reentry Configurations for the Five-Stage Scout Vehicle. NASA TN D-1790, 1963.

6. Johnston, Patrick J.: Longitudinal Aerodynamic Characteristics of Several Fifth-Stage Scout Reentry Vehicles From Mach Number 0.60 to 24.4 Including Some Reynolds Number Effects on Stability at Hypersonic Speeds. NASA TN D-1638, 1963.

7. Frank, Joseph L.; Green, Kendal H.; and Hofstetter, Robert U.: Measurements of the Flow Over Blunt-Nosed Bodies At Mach Numbers From 2.5 to 3.5. NASA TM X-367, 1960.

8. Jackson, Mary W.; and Czarnecki, K. R.: Boundary-Layer Transition on a Group of Blunt Nose Shapes at a Mach Number of 2.20. NASA TN D-932, 1961.

9. Jones, Robert A.: Heat-Transfer and Pressure Distributions on a Flat-Face Rounded-Corner Body of Revolution With and Without a Flap at a Mach Number of 8. NASA TM X-703, 1962.

10. Kemp, Nelson H.; Rose, Peter H.; and Detra, Ralph W.: Laminar Heat Transfer Around Blunt Bodies in Dissociated Air. J. Aero/Space Sci., vol. 26, no. 7, July 1959, pp. 421-430.

11. Romeo, David J.: Experimental Results of the Pressure Distribution on a Blunt-Nose Conical-Afterbody Lunar-Mission Spacecraft With Four Nose-Edge Radii for a Mach Number of 6.0 and an Angle-of-Attack Range of 0° to 50°. NASA TM X-705, 1962.

12. Weinstein, Irving: Heat Transfer and Pressure Distributions on a Hemisphere-Cylinder and a Bluff-Afterbody Model in Methane-Air Combustion Products and in Air. NASA TN D-1503, 1962.

[redacted]

13. Wittliff, Charles E.; and Curtis, James T.: Normal Shock Wave Parameters in Equilibrium Air. Rept. No. CAL-111 (Contract No. AF 33(616)-6579), Cornell Aeron. Lab., Inc., Nov. 1961.

14. Marrone, Paul V.: Normal Shock Waves in Air: Equilibrium Composition and Flow Parameters for Velocities From 26,000 to 50,000 Ft/Sec. CAL Rep. No. AG-1729-A-2 (Contract NASr-119), Cornell Aero. Lab., Inc., Aug. 1962.

15. Hansen, C. Frederick: Approximations for the Thermodynamic and Transport Properties of High-Temperature Air. NASA TR R-50, 1959. (Supersedes NACA TN 4150.)

16. Cooper, Morton; and Mayo, Edward E.: Measurements of Local Heat Transfer and Pressure on Six 2-Inch-Diameter Blunt Bodies at a Mach Number of 4.95 and at Reynolds Numbers Per Foot up to 81×10^6. NASA MEMO 1-3-59L, 1959.

17. Bertram, Mitchel H.; and Everhart, Philip E.: An Experimental Study of the Pressure and Heat-Transfer Distribution on a 70° Sweep Slab Delta Wing in Hypersonic Flow. NASA TR R-153, 1963.

18. Minzner, R. A.; Champion, K. S. W.; and Pond, H. L.: The ARDC Model Atmosphere, 1959. Air Force Surv. in Geophys. No. 115 (AFCRC-TR-59-267), Air Force Cambridge Res. Center, Aug. 1959.

19. Detra, R. W.; Kemp, N. H.; and Riddell, F. R.: Addendum to "Heat Transfer to Satellite Vehicles Re-entering the Atmosphere." Jet Propulsion, vol. 27, no. 12, Dec. 1957, pp. 1256-1257.

20. Kemp, N. H.; and Riddell, F. R.: Heat Transfer to Satellite Vehicles Re-Entering the Atmosphere. Jet Propulsion, vol. 27, no. 2, pt. 1, Feb. 1957, pp. 132-137, 147.

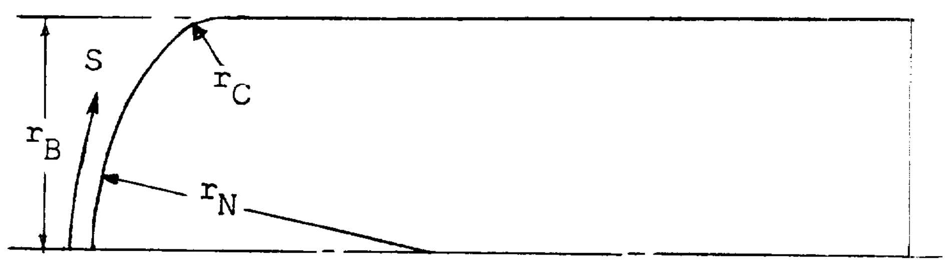

Figure 1.- Sketch of typical blunt body.

[redacted]

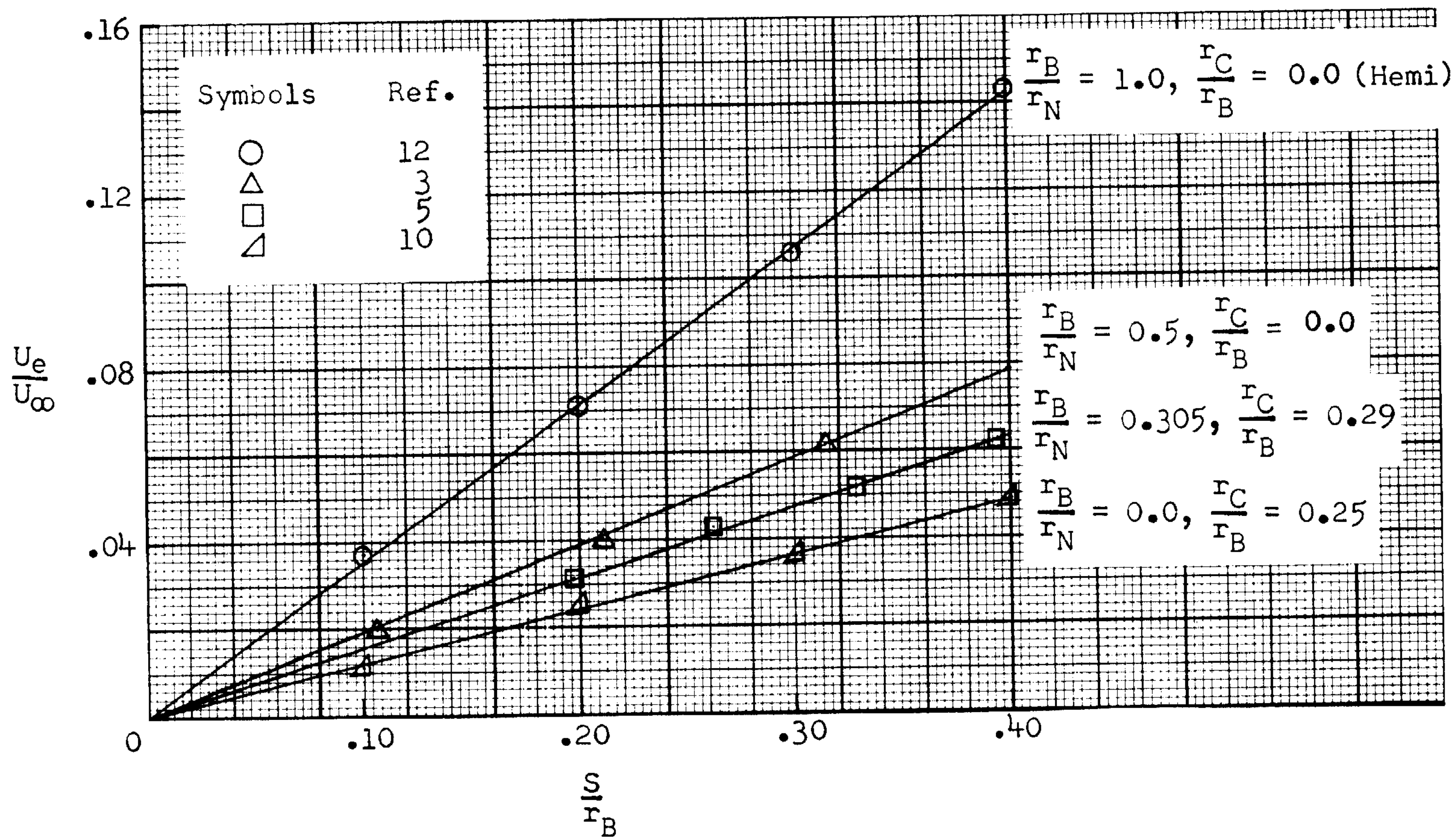

Figure 2.- Typical stagnation-region velocity distributions computed for U_∞ = 23 800 ft/sec and an altitude of 138 000 ft.

[redacted]

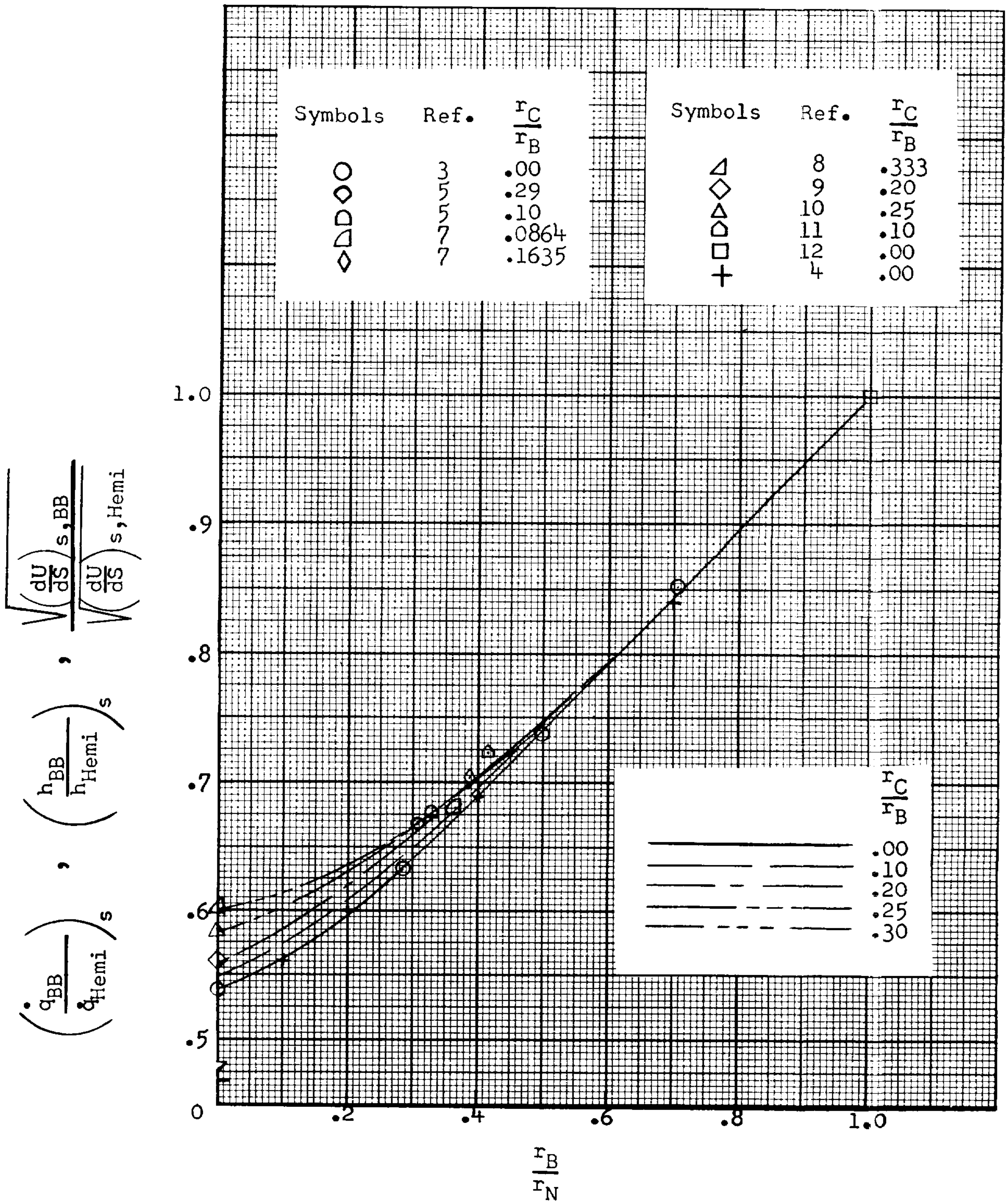

Figure 3.- Stagnation-point heating-rate parameters on hemispherical segments of different curvatures for varying corner-radius ratios.

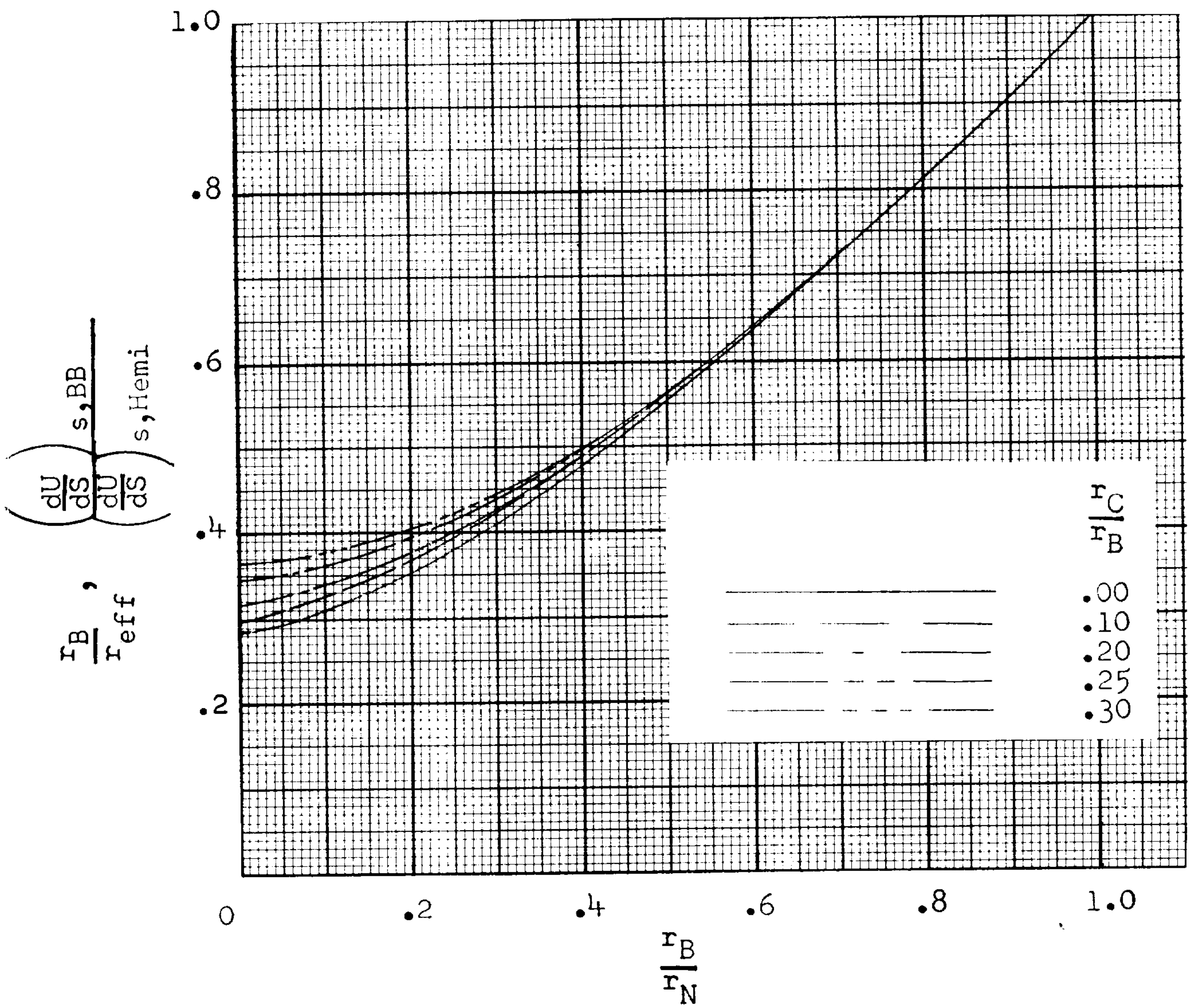

Figure 4.- Variation of effective radius and stagnation-point velocity gradient on hemispherical segments of different curvatures for varying corner radius ratios.

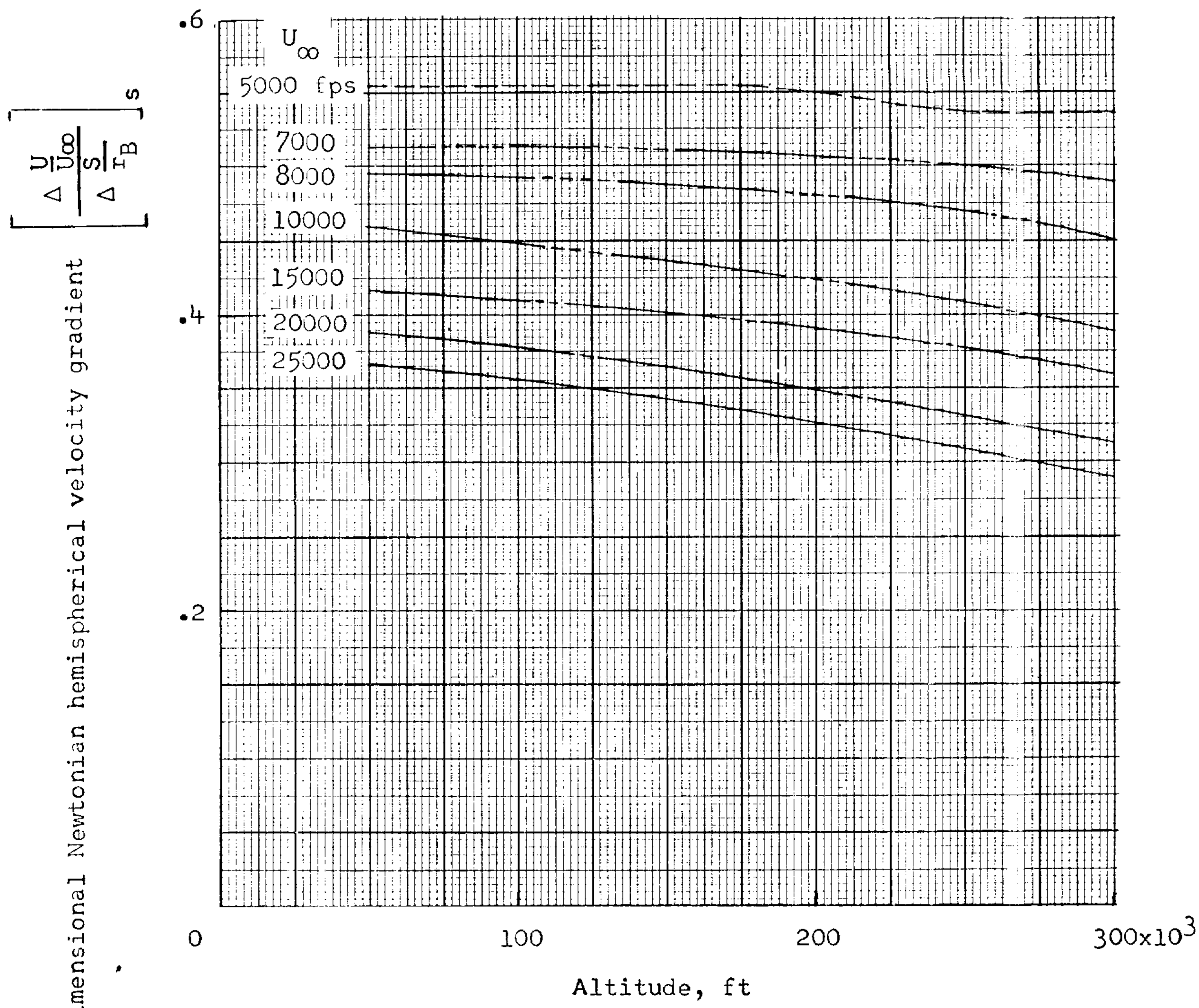

Figure 5.- Nondimensional Newtonian stagnation-point velocity gradient on a hemisphere over a range of altitudes and velocities.

[redacted]

[redacted]